Journal of Advanced Ceramics
2015, **4**(1): 31–38
DOI: 10.1007/s40145-015-0128-2

ISSN 2226-4108
CN 10-1154/TQ

Research Article

Microstructure and mechanical properties of SiC_f/SiBCN ceramic matrix composites

Jiaying WANG, Zhihua YANG, Xiaoming DUAN, Dechang JIA*, Yu ZHOU

Institute for Advanced Ceramics, Harbin Institute of Technology, Harbin 150080, China

Received: August 29, 2014; Accepted: September 17, 2014

Abstract: SiC fiber reinforced SiBCN ceramic matrix composites (CMCs) have been prepared by mechanical alloying and consolidated by hot pressing. During the sintering process, amorphous SiC fibers crystallized seriously and transformed into β-SiC. Meanwhile, the interfacial carbothermal reactions caused the strong bonding between the matrix and fibers. As a result, SiC_f/SiBCN fractured in a typical catastrophic manner. Room-temperature mechanical properties reached the maximums for the CMC samples sintered at 1900 ℃/60 MPa/30 min. The density, flexural strength, Young's modulus and fracture toughness are 2.56±0.02 g/cm^3, 284.3±17.9 MPa, 183.5±11.1 GPa and 2.78±0.14 MPa·m$^{1/2}$, respectively.

Keywords: hot pressing; composites; mechanical properties; fiber

1 Introduction

SiBCN ceramics have been widely investigated due to their better high-temperature properties such as oxidation [1–3] and creep resistance [4,5], which are expected to be applied in aerospace and anti-ablation structures in the future. Recently, various methods to fabricate these novel ceramics have been attempted such as precursor infiltration and pyrolysis (PIP) [6,7], physical vapor decomposition (PVD) [8,9] and mechanical alloying and hot pressing (MA–HP) [10]. However, a general problem of these ceramics is their brittleness, especially utilized under severe thermal shock or ablation environment. Thus, some approaches to reinforce the matrix such as the introduction of fibers are necessary.

Among the reinforcements for precursor derived ceramics, fibers have been widely used in manufacturing the fiber reinforced ceramic matrix [11–14]. By the fiber/matrix debonding and fiber pull-out, elastic strain energy (or the stress field of the crack tip) could be dissipated in this kind of ceramic matrix composites (CMCs). Carbon fibers have usually been chosen as the reinforcements due to their outstanding high-temperature properties. Through the method of polymer impregnation pyrolysis, fiber reinforced ceramic composites could be fabricated by vacuum assisted infiltration of a liquid SiBCN precursor into stacked woven carbon fiber fabrics [12,13]. SiC particles are also utilized to improve the thermal stability of CMCs [15]. Unfortunately, carbon fibers could easily be oxidized in air atmosphere or oxygen contained ablative environment, which would steadily decrease the mechanical properties [16]. Mass ablation rate and linear ablation rate of C_f/SiBCN composites are namely 15.2 mg/s and 0.0455 mm/s under an oxyacetylene torch environment respectively, which are notably more than those of SiC fiber reinforced composites [16]. To improve the ablation

* Corresponding author.
E-mail: dcjia@hit.edu.cn

properties, silicon carbide fibers have been chosen as the reinforcement of SiBCN matrix in our recent research [17].

In this paper, SiC_f/SiBCN CMCs have been prepared by mechanical alloying and hot pressing. Mechanical properties and microstructures of the CMCs were carefully studied, especially the behavior of carbon diffusion in the adjacent area of fibers. These results may be helpful for the choice of coating on SiC fibers and applications of fiber reinforced SiBCN composites.

2 Experimental procedures

2. 1 Amorphous SiBCN powder preparation

Preparation of amorphous SiBCN powder has been discussed in our previous research [18,19]. Crystalline raw materials, namely cubic silicon (45.0 μm, 99.5% in purity, Beijing MounTain Technical Development Center, China), hexagonal boron nitride (0.6 μm, 98.0% in purity, Advanced Technology & Materials Co. Ltd., Beijing, China) and graphite powder (8.7 μm, 99.5% in purity, Qingdao HuaTai Lubricant Sealing S&T Co. Ltd., China) were used as starting materials in the experiment. The composition was designed as Si:C:BN = 2:3:1 in molar ratio. This designation depended on the literature and our previous research to compare with precursor derived ceramics [20]. The ball-to-powder mass ratio was set as 20:1. The powder mixture was loaded in silicon nitride vials along with silicon nitride balls under an argon atmosphere. Sealed with rubber rings, two vials were fixed on a planetary ball mill (Fritsch P4, Germany). The rotation speed of the main disk was set at 350 rpm and the vials 600 rpm in reverse, and the total milling time was 40 h. The milling parameters have been discussed in another previous research paper [19].

2. 2 Fabrication of SiC_f/SiBCN ceramic composites by hot pressing method

The properties of SiC fibers are summarized in Table 1. Before being cut into 1–2 mm in length, the fibers were treated to remove the organics on the surface under 370 ℃/2 h/air. Then the powder and fibers were mixed with ethanol by ball milling for 4 h. The mixture was dried and hot pressed in HIGH MULTI 1000 furnace. The mixture was heated to a set sintering temperature (1800 ℃ or 1900 ℃) under a heating rate of 20 ℃/min, and then kept at the target temperature and pressure in the nitrogen atmosphere (1 bar) for 30 min or 60 min. The loading process of the axial pressure started at 1200 ℃ and finished at 1400 ℃. During the cooling stage, the pressure was slowly unloaded in 5 min. The sintering methods and serial numbers are listed in Table 2.

Table 1 Parameters of SLFC1 SiC fibers adopted in the current research

Raw fiber	Density (g/cm^3)	Fiber diameter (μm)	Tensile strength (GPa)	Young's modulus (GPa)
SLFC1	2.36	13±0.5	1.5±1.0	140±10

2. 3 Microstructure and property characterization

For the phase identification, X-ray diffractometer (40 kV/100 mA, D/max-γB Cu Kα, Rigaku Corporation, Japan) was used to obtain the X-ray diffraction (XRD) spectra at $2\theta = 10°–90°$ with a scanning speed of 4 (°)/min. The as-milled SiBCN powder and fracture morphologies of the ceramics were observed by scanning electron microscopy (SEM, 30 kV, Quanta 200FEG, FEI Co., USA). The microstructure and energy dispersive X-ray spectroscopy (EDX) analysis were conducted on the transmission electron microscope (Tecnai G^2 F30, 300 kV, FEI Co., USA).

The property measurement was carried out on omnipotence mechanics tester (Instron 5569, Instron Co., USA). Flexural strength and Young's modulus were obtained using three-point bending test on 3 mm × 4 mm × 32 mm bars with a span of 20 mm and a crosshead speed of 0.5 mm/min. Fracture toughness was tested on 2 mm × 4 mm × 20 mm bars with a span of 16 mm and a crosshead speed of 0.05 mm/min.

3 Results and discussion

3. 1 Characterizations of amorphous powder

Crystalline raw powder has been completely decrystallized after 40 h milling from the XRD pattern as shown in Fig. 1. Through the crash between silicon

Table 2 Sintering method and serial number of SiC_f/SiBCN composite specimens

Serial number	Sintering method		
	Sintering temperature (℃)	Pressure (MPa)	Holding time (min)
180060	1800	60	30
190040	1900	40	30
19006030	1900	60	30
19006060	1900	60	60

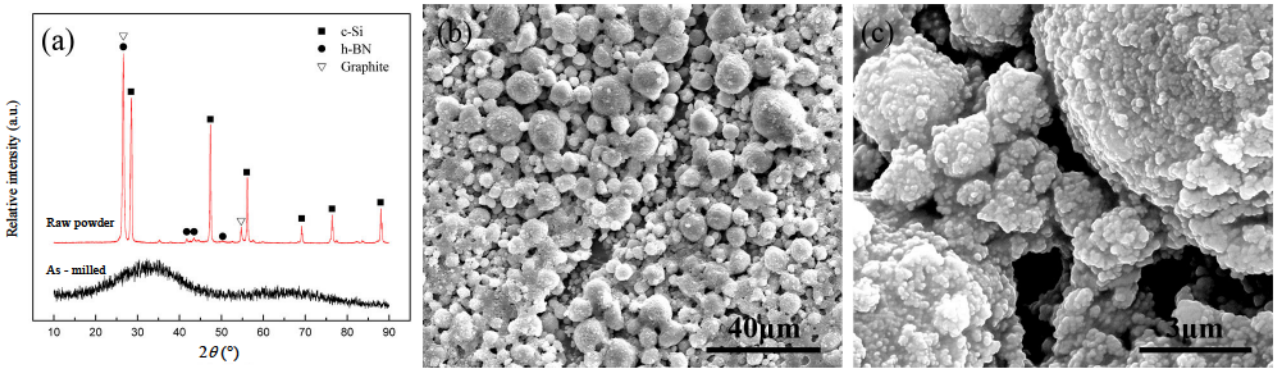

Fig. 1 (a) XRD analysis of raw powder mixture and as-milled amorphous SiBCN powder; (b) and (c) surface morphology of SiBCN powder by mechanical alloying process.

nitride vitals and balls, physical and chemical reactions including fierce collisions, rupture, local temperature, fusion and short-range collisions, happen during high-energy mechanical alloying. Meanwhile, in Fig. 1(b), the amorphous powder is composed by numerous near-spherical agglomerates. In our previous research, these agglomerates are formed by nano particles, whose grain sizes are statistically 116±34 nm by transmission electron microscopy (TEM) analysis. More information about the amorphous powder, such as physical and surface characteristics, has been described in other research papers [18,19].

3. 2 Microstructures of SiC_f/SiBCN composites

After hot pressing, the mixture of short SiC fibers and SiBCN amorphous powder has crystallized seriously. The ceramic matrix consists of α-SiC, β-SiC and BNC phases (Fig. 2). When the sintering temperature rises from 1800 ℃ to 1900 ℃, the diffraction peaks exhibit a reduced full width at half maximum (FWHM) and increased peak intensity, implying higher crystal content. Meanwhile, it reveals that β-SiC phase tends to transform to α-SiC, according to the relative intensities of SiC phases. Similar results are also obtained when the sintering pressure or holding time are further increased.

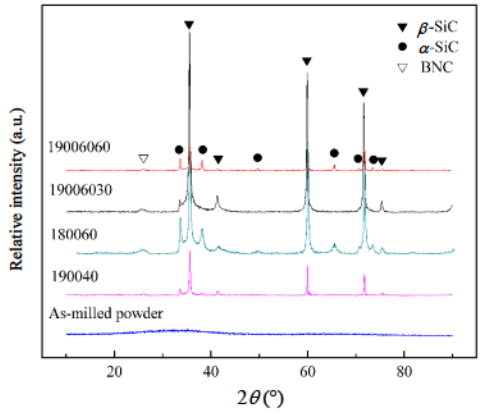

Fig. 2 XRD analysis of SiC_f/SiBCN composites under different sintering conditions.

Figure 3(a) gives the TEM microstructures of the SiC_f/SiBCN matrix prepared at 1900 ℃/60 MPa/60 min. The composite matrix mainly consists of nano-sized SiC and BNC grains. SiC grain size is about 100 nm as shown in Fig. 3(a). Meanwhile, BNC phases primarily distribute in the interphase of SiC grains and limit SiC grain growth [20]. However, it is difficult to observe the morphology of SiC fibers because the contrast of the composite matrix is similar with SiC fibers. Thanks to EDX spectrum, SiC fiber region is found in the composites sintered at 1800 ℃/60 MPa/30 min. SiC fibers were severely crystallized and the size of SiC grain is about 100 nm after hot pressing (Figs. 3(b) and 3(c)).

Unfortunately, because the only difference between the matrix and fiber of bright field image is the existence of BNC interphase, the boundary between matrix and fiber is hard to be observed by TEM. More researches about the boundary would be reported in our further research.

3. 3 Interfacial carbothermal reactions in SiC_f/SiBCN composites during the sintering process

Figure 4 indicates the fractured surface morphologies of SiC_f/SiBCN composites prepared at 1900 ℃/60 MPa/30 min. Layer-fractured phenomenon of SiC fiber could be generally found in the fractured surface. Protrusions or pits exist in the center part of SiC fiber and the thickness of fractured layer is about 2 μm, which equals to the SiC sheath shown in Fig. 4(a). Meanwhile, on the fractured surface of composites prepared at 1900 ℃/60 MPa/60 min, similar phenomenon could be observed as well but the

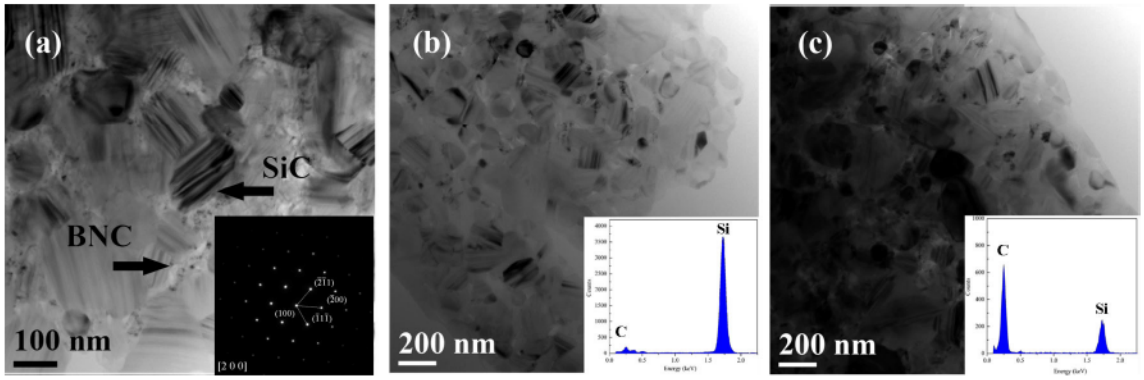

Fig. 3 (a) Bright field image and SAED pattern (inset) of SiC_f/SiBCN CMCs prepared at 1900 ℃/60 MPa/60 min; (b) and (c) microstructures and EDX analysis of SiC fibers in SiC_f/SiBCN composites prepared at 1800 ℃/60 MPa/30 min in different areas.

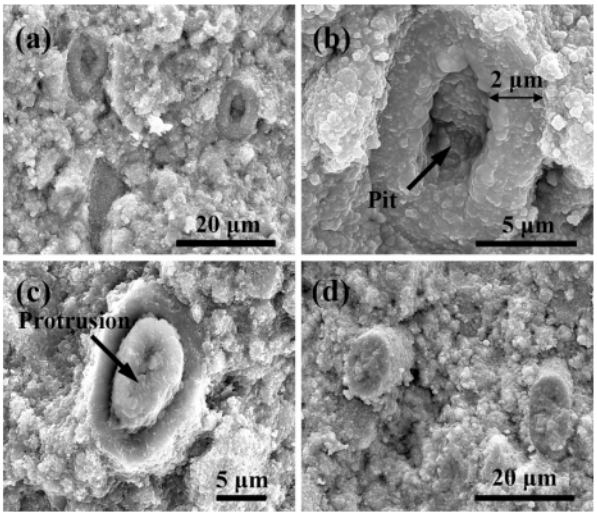

Fig. 4 Layer-fractured phenonemon in the SiC_f/SiBCN composites prepared at 1900 ℃/60 MPa/30 min and 60 min: (a) pits in the center of SiC fibers; (b) thickness of react layer; (c) protrusions in the center of SiC fibers; (d) morphology of fractured surface prepared at 1900 ℃/60 MPa/60 min.

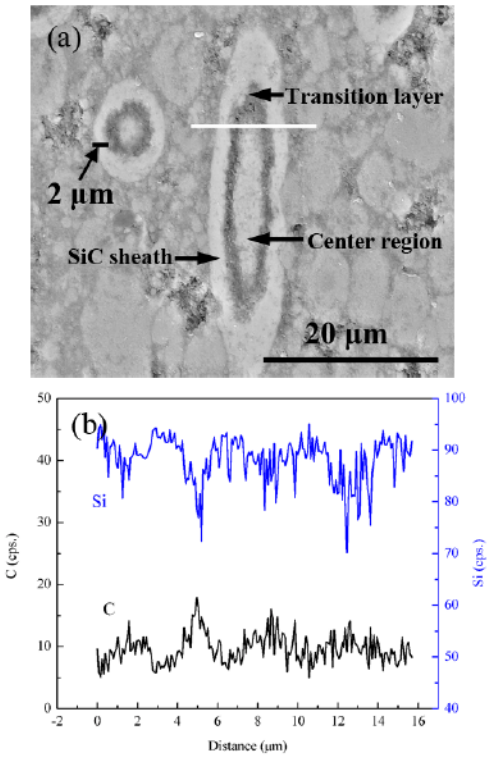

Fig. 5 Uniform distribution of carbon in the adjacent area of fibers: (a) electron back-scattered diffraction (EBSD) analysis of SiC_f/SiBCN composite surface; (b) line scanning in Fig. 5(a).

thickness increases and few protrusions or pits are left in the center area of the fiber. Between the edge and center of SiC fiber, there also exists a low-density layer.

Element analysis by line scanning around the fiber's adjacent area has been shown in Fig. 5. Three regions could be apparently observed from the outsides and insides, namely, SiC sheath, transition layer and center region. In the SiC sheath and center region, the content of carbon is significantly higher than that of transition layer. Meanwhile, the obvious carbon gradient exists in the fiber area. EDX spectra of fiber's different areas by TEM show the same result (Figs. 3(b) and 3(c)) as the line scanning analysis. Based on the results above, it can be inferred that chemical reactions happen during the sintering process and cause carbon diffusion in the adjacent area of fibers.

SiC_xO_y and excess carbon in the SiC fibers and amorphous SiBCN powder are the main reason causing the carbon diffusion during the sintering process. SiC fibers applied in the experiments are similar with the first generation of Nicalon SiC fibers (Tokyo, Japan). During the curing process of fiber preparation, a large amount of oxygen (~1%) is introduced [21]. After the pyrolysis in the nitrogen atmosphere, fibers are composited of silicon, carbon and oxygen which form the amorphous SiC_xO_y phase. Assisted by X-ray

photoelectron spectroscopy (XPS) spectrum, the elemental and chemical analysis of fibers reflects that Nicalon fiber is a continuous SiC and SiC_xO_y tetrahedron network with an excess of carbon and exhibits a silica sheath according to the SiC_xO_y bonding at 102.5 eV which is intermediate between SiC and SiO_2 [22–25].

On the other hand, excess carbon, or free carbon, also influences interfacial microstructures between fibers and matrix. SiC fibers have been heat treated in 370 ℃ for 2 h to improve the dispersity of fibers in our research. The carbon in the out layer of fibers would react with oxygen and the content of free carbon decreases to cause SiO_2 or SiC_xO_y formed. Besides, free carbon also exists in amorphous SiBCN powder because the powder is fabricated by mechanical alloying and raw powder includes graphite. Related results have been reported in our other research paper [18]. Thus, free carbon in the fibers and powder would react with SiO_2 and cause the strong bonding between fibers and matrix.

According to previous work and our analysis, we summarize the schematic of carbon diffusion and layer-fractured formation in Fig. 6. Carbon diffusion in the SiC_f/SiBCN ceramic composites is attributed to the carbothermal reactions between the free carbon and silica or silicon monoxide. The interfacial carbothermal reactions provide the diffusion drive and cause the gradient of carbon. In the first step from 1000 ℃ to 1500 ℃, the SiC_xO_y phase would partly decompose to SiC and SiO_2, and β-SiC crystals would be left during this process as shown in Fig. 6(b) [26]. When the sintering temperature rises to 1500 ℃, carbothermal reactions would happen and porous SiC transition layer would be formed on the surface of SiC fibers. If the temperature reaches above 1600 ℃, free carbon would react with the silicon monoxide produced by the decomposition of SiC_xO_y phase and form the SiC sheath on the transition layer accompanying with the carbothermal reactions [27]. Possible reactions related to the gas formation are as follows:

$$SiO_2(s)+3C(s) \rightarrow SiC(s)+2CO(g) \quad (1)$$

$$SiC_xO_y(s) \rightarrow \frac{x-y+1}{2}SiC(s)+\frac{y-x+1}{2}SiO(g)+\frac{x+y-1}{2}CO(g) \quad (2)$$

$$SiO(g)+C(s) \rightarrow SiC(s)+CO(g) \quad (3)$$

$$2SiO(g)+3C(s) \rightarrow 2SiC(s)+CO_2(g) \quad (4)$$

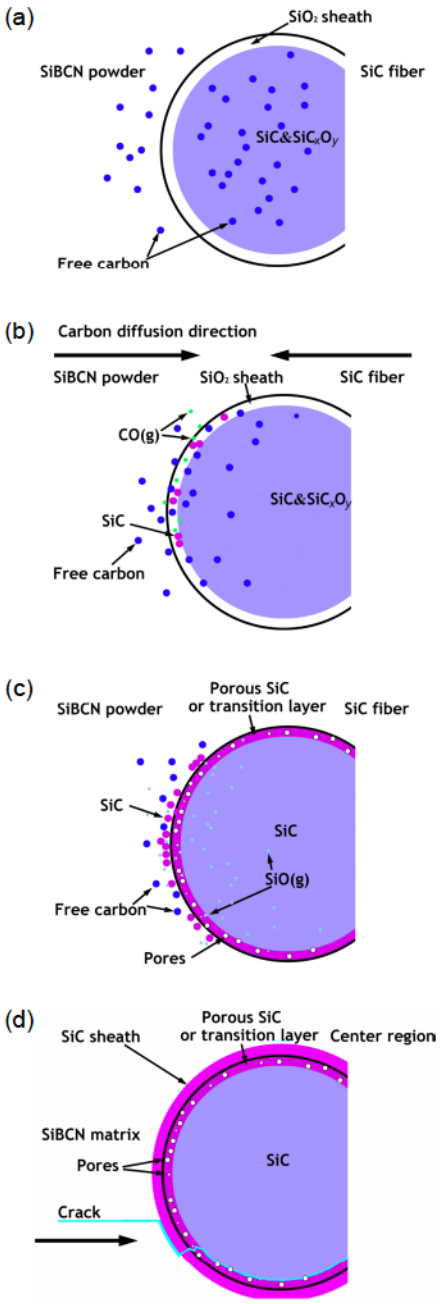

Fig. 6 Schematic of carbon diffusion and layer-fractured phenomenon in the SiC_f/SiBCN composites.

The above reactions have been confirmed by experimental data and thermodynamics. The release of gas, such as CO, SiO and CO_2, causes the porous transition layer. Reactions (2), (3) and (4) are the reasons which obtain the formation of SiC sheath. The formation of SiC sheath and the calculation of thermodynamics could not indicate that the reactions could be possessed during the sintering process but prove the theory of re-deposition of SiC grains on the surface of SiC fibers as Honstein *et al*. proposed [27].

3. 4 Mechanical properties of SiC_f/SiBCN ceramic composites

Figure 7 shows the typical fractured behavior of SiC_f/SiBCN ceramic composites. Unfortunately, the fractured behavior of composites is catastrophic brittle manner and the introduction of short SiC fibers could not change the fractured behavior due to SiC fiber crystallization and the strong interfacial bonding between SiC fibers and the matrix. When the crack propagates to SiC fibers, crack deflection cannot take place and it tends to directly cut through the interphase of SiC grains. These situations are also reflected from the fractured surface of three-point bending specimen as illustrated in Fig. 8. Except the specimen prepared at 1900 ℃/60 MPa/30 min, no fiber pull-out could be observed on the fractured surfaces. Meanwhile, in the specimen prepared at 1900℃/60 MPa/30 min, the length of fiber pull-out is short so the toughening effect from the SiC fibers could not be insured. Further researches about BN weak layer have been surveyed in our other research paper in the future.

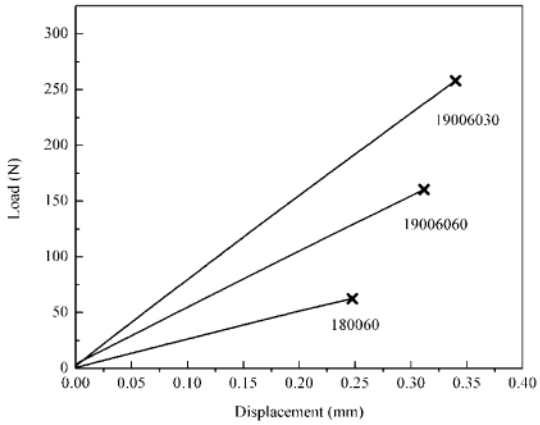

Fig. 7 Typical fractured behaviors of SiC_f/SiBCN composites at different sintering methods.

Table 3 summarizes the room-temperature mechanical properties and average thermal expansion coefficient of SiC_f/SiBCN ceramic composites. The average thermal expansion coefficient of SiC_f/SiBCN ceramic composites is slightly lower than that of the pure MA-SiBCN ceramic, whose thermal expansion coefficient is about 4.7×10^{-6} $(℃)^{-1}$. In the three-point bending fractured surface of specimen prepared at 1800 ℃/60 MPa/30 min, the density of matrix is low and micro-defects in the matrix limit the mechanical properties of composites. With the increase of sintering parameters such as sintering temperature, pressure and holding time, the density of matrix improves notably and mechanical properties improve as well. Mechanical properties reach the maximum values after hot pressing at 1900 ℃/60 MPa/30 min. The ceramic composite has room-temperature density, flexural strength, Young's modulus and fracture toughness of 2.56±0.02 g/cm^3, 284.3±17.9 MPa, 183.5±11.1 GPa and 2.78±0.14 MPa·m$^{1/2}$, respectively. Compared with our previous research about carbon fiber reinforced SiBCN matrix, the mechanical properties improve

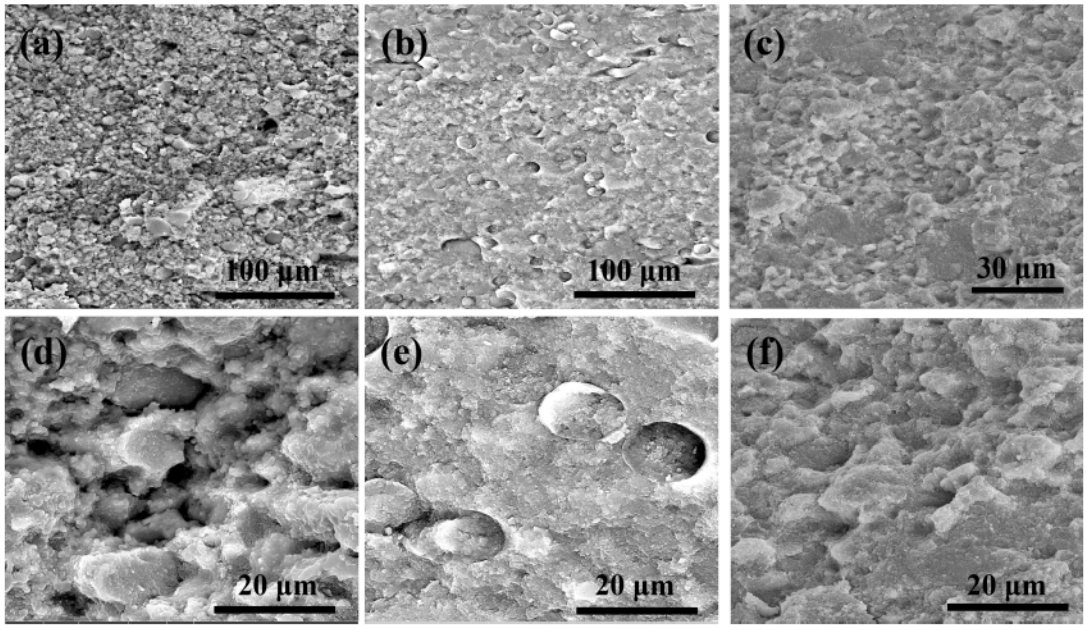

Fig. 8 Morphology of fractured surfaces of SiC_f/SiBCN composites prepared at different sintering methods: (a) and (d) 1800 ℃/60 MPa/30 min; (b) and (e) 1900 ℃/60 MPa/30 min; (c) and (f) 1900 ℃/60 MPa/60 min.

Table 3 Room-temperature properties of SiC_f/SiBCN composites hot pressed at different sintering methods

Serial number	Density ρ (g/cm^3)	Flexural strength σ (MPa)	Fracture toughness K_{IC}, (MPa·m$^{1/2}$)	Young's modulus E (GPa)
180060	2.35±0.01	73.3±2.4	1.04±0.11	73.3±3.0
190040	2.46±0.02	70.2±6.3	1.72±0.11	64.1±2.8
19006030	2.56±0.02	284.3±17.9	2.78±0.14	183.5±11.1
19006060	2.57±0.01	171.8±6.5	3.66±0.08	107.3±7.3

notably. However, flexural strength of the specimen prepared at 1900 ℃/60 MPa/60 min is decreased compared with that prepared at 1900 ℃/60 MPa/30 min and fracture toughness is increased. On the fractured surface of the specimen prepared at 1900 ℃/60 MPa/60 min, reactions between the matrix and fibers occur seriously and no fiber pull-out could be observed but some pits could be found. The size and shape of pits are different with SiC fiber pull-out pits, as shown in Fig. 8(f). Maybe SiC grains in the matrix grow with the holding time increasing. SiC grain pull-out could also improve the fracture toughness of SiC_f/SiBCN composites.

3.5 Relations between interfacial carbothermal reactions and mechanical properties of SiC_f/SiBCN composites

Apparently, interfacial carbothermal reactions decrease the mechanical properties of SiC_f/SiBCN composites at room temperature, especially the reinforcement of SiC fibers. The reactions between free carbon and SiO_2 sheath of as-prepared SiC fibers would cause the strong bonding between the matrix and fibers. It makes the fibers hard to be debonded from the matrix when the composites are fractured. Meanwhile, the formation of porous transition layer is attributed to gases emitting such as SiO(g), CO(g) and CO_2(g) during the sintering process. It also causes the degradation of SiC fibers. When the crack propagates through the SiC sheath, the crack could easily deflect in the transition layer and form the layer-fractured phenomenon.

Nowadays, similar results about the carbothermal reactions or porous layer between fibers and matrix during the sintering process have been investigated by other research groups as well. Layer-fractured phenomenon could be found in the SiC_f/SiC ceramic composites prepared by chemical vapor infiltration (CVI), in which SiC fibers have been coated by PIP-SiC [28]. Because of the weak bonding between CVI-SiC and PIP-SiC, the fractured surface of SiC also reflects the same phenomenon of these experiments. Chen *et al*. [21] also pointed out that the oxygen picked up during the oxidation curing would influence the stoichiometry of sinter SiC fibers and the evolution of CO, CO_2 and SiO generates high porosity. Aluminum or Al/B sintering additives have been introduced to the fibers as sintering additives improve the densification of fibers. To sum up, carbothermal reactions lead to the strong bonding and porosity layer between the matrix and fibers at the same time, which decrease the reinforcement of fibers.

To improve the properties of SiC_f/SiBCN composites, the methods to prevent the carbothermal reactions and ameliorate the bonding between matrix and fibers are necessary to be carried out. Other relative researches such as BN coating on the fiber to restrict the carbothermal reactions and improve the reinforcement of SiC fibers would be accomplished in our future research.

4 Conclusions

SiC_f/SiBCN ceramic composites were fabricated by hot pressing under different sintering conditions. Similar with the pure SiBCN matrix, the phases of SiC_f/SiBCN composite matrix are α-SiC, β-SiC and BNC whose size is about 100 nm. However, during the sintering process, SiC fibers crystallize seriously and degrade, which is not beneficial to their strengthening effects.

Carbothermal reactions during the sintering process cause the layer-fractured phenomenon and decrease the mechanical properties of SiC_f/SiBCN composites at room temperature. The excess carbon in the powder and fibers would react with SiO_2 on the surface of fibers and the reaction layer mainly consists of SiC during the sintering process. The reactions would further cause the strong bonding between the matrix and fibers and make the composite fracture in a brittle manner. Meanwhile, with the release of gases such as SiO(g), CO(g) and CO_2(g), micro defects in the transition layer would be left. When the crack spreads to the transition layer, it would slightly deflect in the layer and form the layer-fractured phenomenon in the fractured surfaces of specimens.

SiC_f/SiBCN composite prepared at 1900 ℃/60 MPa/30 min shows relatively excellent room-temperature mechanical properties, with the density, flexural strength, Young's modulus and fracture toughness of 2.56±0.02 g/cm^3, 284.3±17.9 MPa, 183.5±11.1 GPa and 2.78±0.14 MPa·m$^{1/2}$, respectively.

Acknowledgements

This work has been supported by the National Natural Science Funds for Distinguished Young Scholar of China under Grant No. 51225203. This work was also supported by the National Natural Science Foundation of China under Grant Nos. 51072041, 50902031 and 51021002. The authors also appreciated the meaningful comments from Dr. Pengfei Zhang.

References

[1] Colombo P, Mera G, Riedel R, *et al*. Polymer-derived ceramics: 40 years of research and innovation in advanced ceramics. *J Am Ceram Soc* 2010, **93**: 1805–1837.

[2] Schiavon MA, Sorarù GD, Yoshida IVP. Poly (borosilazanes) as precursors of Si–B–C–N glasses: Synthesis and high temperatures properties. *J Non-Cryst Solids* 2004, **348**: 156–161.

[3] Weinmann M, Schuhmacher J, Kummer H, *et al*. Synthesis and thermal behavior of novel Si–B–C–N ceramic precursors. *Chem Mater* 2000, **12**: 623–632.

[4] Christ M, Thurn G, Weinmann M, *et al*. High-temperature mechanical properties of Si–B–C–N-precursor-derived amorphous ceramics and the applicability of deformation models developed for metallic glasses. *J Am Ceram Soc* 2000, **83**: 3025–3032.

[5] Kumar NVR, Prinz S, Cai Y, *et al*. Crystallization and creep behavior of Si–B–C–N ceramics. *Acta Mater* 2005, **53**: 4567–4578.

[6] Riedel R, Ruswisch LM, An LN, *et al*. Amorphous silicoboron carbonitride ceramic with very high viscosity at temperatures above 1500 ℃. *J Am Ceram Soc* 1998, **81**: 3341–3344.

[7] Widgeon S, Mera G, Gao Y, *et al*. Effect of precursor on speciation and nanostructure of SiBCN polymer-derived ceramics. *J Am Ceram Soc* 2013, **96**: 1651–1659.

[8] Vijayakumar A, Todi RM, Sundaram KB. Effect of N_2/Ar gas mixture composition on the chemistry of SiCBN thin films prepared by RF reactive sputtering. *J Electrochem Soc* 2007, **154**: H271–H274.

[9] Vishnyakov VM, Ehiasarian AP, Vishnyakov VV, *et al*. Amorphous boron containing silicon carbo-nitrides created by ion sputtering. *Surf Coat Technol* 2011, **206**: 149–154.

[10] Yang Z-H, Zhou Y, Jia D-C, *et al*. Microstructures and properties of $SiB_{0.5}C_{1.5}N_{0.5}$ ceramics consolidated by mechanical alloying and hot pressing. *Mat Sci Eng A* 2008, **489**: 187–192.

[11] Weinmann M, Kamphowe TW, Schuhmacher J, *et al*. Design of polymeric Si–B–C–N ceramic precursors for application in fiber-reinforced composite materials. *Chem Mater* 2000, **12**: 2112–2122.

[12] Lee SH, Weinmann M, Aldinger F. Processing and properties of C/Si–B–C–N fiber-reinforced ceramic matrix composites prepared by precursor impregnation and pyrolysis. *Acta Mater* 2008, **56**: 1529–1538.

[13] Lee S-H, Weinmann M. C_{fiber}/SiC_{filler}/Si–B–C–N_{matrix} composites with extremely high thermal stability. *Acta Mater* 2009, **57**: 4374–4381.

[14] Lee S-H, Weinmann M, Aldinger F. Fabrication of fiber-reinforced ceramic composites by the modified slurry infiltration technique. *J Am Ceram Soc* 2007, **90**: 2657–2660.

[15] Lee S-H, Weinmann M, Gerstel P, *et al*. Extraordinary thermal stability of SiC particulate-reinforced polymer-derived Si–B–C–N composites. *Scripta Mater* 2008, **59**: 607–610.

[16] Zhang P, Jia D, Yang Z, *et al*. Progress of a novel non-oxide Si–B–C–N ceramic and its matrix composites. *J Adv Ceram* 2012, **1**: 157–178.

[17] Wang J, Duan X, Yang Z, *et al*. Ablation mechanism and properties of SiC_f/SiBCN ceramic composites under an oxyacetylene torch environment. *Corros Sci* 2014, **82**: 101–107.

[18] Zhang P, Jia D, Yang Z, *et al*. Physical and surface characteristics of the mechanically alloyed SiBCN powder. *Ceram Int* 2012, **38**: 6399–6404.

[19] Zhang P, Jia D, Yang Z, *et al*. Influence of ball milling parameters on the structure of the mechanically alloyed SiBCN powder. *Ceram Int* 2013, **39**: 1963–1969.

[20] Zhang P, Jia D, Yang Z, *et al*. Crystallization and microstructural evolution process from the mechanically alloyed amorphous SiBCN powder to the hot-pressed nano SiC/BN(C) ceramic. *J Mater Sci* 2012, **47**: 7291–7304.

[21] Chen L, Zhang L, Cai Z, *et al*. Effects of oxidation curing and sintering additives on the formation of polymer-derived near-stoichiometric silicon carbide fibers. *J Am Ceram Soc* 2008, **91**: 428–436.

[22] Schreck P, Vix-Guterl C, Ehrburger P, *et al*. Reactivity and molecular structure of silicon carbide fibres derived from polycarbosilanes. *J Mater Sci* 1992, **27**: 4237–4242.

[23] Schreck P, Vix-Gguterl C, Ehrburger P, *et al*. Reactivity and molecular structure of silicon carbide fibres derived from polycarbosilanes. *J Mater Sci* 1992, **27**: 4243–4246.

[24] Ponthieu C, Marhic C, Lancin M, *et al*. SIMS, EDX, EELS, AES, XPS study of interphases in nicalon fibre–LAS glass matrix composites II. *J Mater Sci* 1994, **29**: 4535–4544.

[25] Lancin M, Ponthieu C, Marhic C, *et al*. SIMS, EDX, EELS, AES, XPS study of interphases in nicalon fibre–LAS glass matrix composites I. *J Mater Sci* 1994, **29**: 3759–3766.

[26] Bois L, Maquet J, Babonneau F, *et al*. Structural characterization of sol–gel derived oxycarbide glasses. 2. Study of the thermal stability of the silicon oxycarbide phase. *Chem Mater* 1995, 7: 975–981.

[27] Honstein G, Chatillon C, Baillet F. Thermodynamic approach to the vaporization and growth phenomena of SiC ceramics. I. SiC and SiC–SiO_2 mixtures under neutral conditions. *J Eur Ceram Soc* 2012, **32**: 1117–1135.

[28] Ding D, Zhou W, Luo F, *et al*. Mechanical properties and oxidation resistance of SiC_f/CVI–SiC composites with PIP–SiC interphase. *Ceram Int* 2012, **38**: 3929–3934.